Title

High Frequency of Gamma Interferon-Producing PLZFloRORγtlo Invariant Natural Killer 1 Cells Infiltrating Herpes Simplex Virus 1-Infected Corneas Is Associated with Asymptomatic Ocular Herpesvirus Infection.

Journal

Journal of Virology, 94(9)

ISSN

0022-538X

Authors

Dhanushkodi, Nisha R
Srivastava, Ruchi
Prakash, Swayam
et al.

Publication Date

2020-04-16

DOI

10.1128/jvi.00140-20

Peer reviewed

AMERICAN SOCIETY FOR MICROBIOLOGY | Journal of Virology®

PATHOGENESIS AND IMMUNITY

High Frequency of Gamma Interferon-Producing PLZF^{lo}RORγt^{lo} Invariant Natural Killer 1 Cells Infiltrating Herpes Simplex Virus 1-Infected Corneas Is Associated with Asymptomatic Ocular Herpesvirus Infection

Nisha R. Dhanushkodi,[a] Ruchi Srivastava,[a] Swayam Prakash,[a] Soumyabrata Roy,[a] Pierre-Gregoire A. Coulon,[a] Hawa Vahed,[a] Angela M. Nguyen,[a] Stephanie Salazar,[a] Lan Nguyen,[a] Cassandra Amezquita,[a] Caitlin Ye,[a] Vivianna Nguyen,[a] Lbachir BenMohamed[a,b,c]

[a]Laboratory of Cellular and Molecular Immunology, Gavin Herbert Eye Institute, University of California, Irvine, School of Medicine, Irvine, California, USA
[b]Department of Molecular Biology and Biochemistry, University of California, Irvine, School of Medicine, Irvine, California, USA
[c]Institute for Immunology, University of California, Irvine, School of Medicine, Irvine, California, USA

ABSTRACT Invariant natural killer (iNKT) cells are among the first innate immune cells to elicit early protective immunity that controls invading viral pathogens. The role of the iNKT cell subsets iNKT1, iNKT2, and iNKT17 in herpesvirus immunity remains to be fully elucidated. In this study, we examined the protective role of cornea-resident iNKT cell subsets using the mouse model of ocular herpesvirus infection and disease. Wild-type (WT) C57BL/6 (B6) mice and CD1d knockout (KO) mice were infected ocularly with herpes simplex virus 1 (HSV-1) (strain McKrae). Cornea, spleen, and liver were harvested at 0, 2, 5, 8, and 14 days postinfection (p.i.), and the frequency and function of the three major iNKT cell subsets were analyzed and correlated with symptomatic and asymptomatic corneal herpesvirus infections. The profiles of 16 major pro- and anti-inflammatory cytokines were analyzed in corneal lysates using Western blot and Luminex assays. Early during ocular herpesvirus infection (i.e., day 2), the gamma interferon (IFN-γ)-producing PLZF^{lo}RORγt^{lo} (promyelocytic leukemia zinc finger, retinoic acid-related orphan receptor gT) iNKT1 cell subset was the predominant iNKT cell subset in infected asymptomatic corneas. Moreover, compared to the asymptomatic corneas of HSV-1-infected WT mice, the symptomatic corneas CD1d KO mice, with iNKT cell deficiency, had increased levels of the inflammatory cytokine interleukin-6 (IL-6) and decreased levels of IL-12, IFN-γ, and the JAK1, STAT1, NF-κB, and extracellular signal-regulated kinase 1/2 (ERK1/2) pathways. Our findings suggest that IFN-γ-producing PLZF^{lo}RORγt^{lo} iNKT1 cells play a role in the protective innate immune response against symptomatic ocular herpes.

IMPORTANCE We investigated the protective role of iNKT cell subsets in asymptomatic ocular herpesvirus infection. We found that early during ocular herpesvirus infection (i.e., on day 2 postinfection), IFN-γ-producing PLZF^{lo}RORγt^{lo} iNKT1 cells were the predominant iNKT cell subset in infected corneas of asymptomatic B6 mice (with little to no corneal herpetic disease), compared to corneas of symptomatic mice (with severe corneal herpetic disease). Moreover, compared to asymptomatic corneas of wild-type (WT) B6 mice, the symptomatic corneas of CD1d KO mice, which lack iNKT cells, showed (i) decreases in the levels of IFN-γ and IL-12, (ii) an increase in the level of the inflammatory cytokine IL-6; and (iii) downregulation of the JAK1, STAT1, NF-κB, and ERK1/2 pathways. The findings suggest that early during ocular herpesvirus infection, cornea-resident IFN-γ-producing PLZF^{lo}RORγt^{lo} iNKT1 cells provide protection from symptomatic ocular herpes.

Citation Dhanushkodi NR, Srivastava R, Prakash S, Roy S, Coulon P-GA, Vahed H, Nguyen AM, Salazar S, Nguyen L, Amezquita C, Ye C, Nguyen V, BenMohamed L. 2020. High frequency of gamma interferon-producing PLZF^{lo}RORγt^{lo} invariant natural killer 1 cells infiltrating herpes simplex virus 1-infected corneas is associated with asymptomatic ocular herpesvirus infection. J Virol 94:e00140-20. https://doi.org/10.1128/JVI.00140-20.

Editor Jae U. Jung, University of Southern California

Address correspondence to Lbachir BenMohamed, Lbenmoha@uci.edu.

This work is dedicated to the memory of the late Steven L. ("Steve") Wechsler (1948 to 2016), whose numerous pioneering works on herpes infection and immunity laid the foundation for this line of research.

Received 27 January 2020
Accepted 13 February 2020
Accepted manuscript posted online 26 February 2020
Published 16 April 2020

KEYWORDS HSV-1, ocular infection, herpes, iNKT cells, DC, CD1d knockout mice, asymptomatic, symptomatic

Herpes simplex virus 1 (HSV-1) is among the most prevalent and successful human pathogens (1). HSV-1 infects over 3.72 billion individuals worldwide and can cause potentially blinding recurrent corneal keratitis (1–7). Both innate and adaptive immune cell subsets are necessary to combat HSV-1 infection and disease (8–11). Innate immune cells are rapid responders and play a critical role in early host protective immune responses that control virus replication (12). One such cell type is natural killer T (NKT) cells participating in the defense against viral pathogens, including HSV-1 (13–15). NKT cells, as the name suggests, share phenotypic and functional features of both NK and T cells and, unlike other cells, migrate from the thymus, primed to respond to and aid in early antiviral defenses (16). Invariant natural killer T (iNKT) cells are type 1 NKT cells that express a semi-invariant T cell receptor (TCR) consisting of a limited number of Vβ chains associated with an invariant TCR α-chain, Vα14Jα18 in mice and Vα24Jα18 in humans (17–23). The iNKT TCRs can detect lipid antigens bound to a major histocompatibility complex (MHC) class I-like molecule, called CD1d, present on antigen-presenting cells (APCs) such as dendritic cells (DCs), B cells, macrophages, and epithelial cells (12). iNKT cells function mostly by the rapid release of cytokines and lead to the stimulation or suppression of immune reactions (12, 24–27). Exogenously added α-galactosylceramide (αGalCer) (a synthetic glycolipid originally derived from a marine sponge) binds to CD1d acting as a potent stimulator of iNKT cells, resulting in the rapid release of huge amounts of cytokines such as gamma interferon (IFN-γ) or interleukin-4 (IL-4) (28–30).

iNKT cells are among the innate immune cells that play an early critical role in eliciting protective immunity that controls virus replication. Although there are currently no known herpesvirus-associated lipid iNKT antigens, iNKT activation can occur in the absence of a pathogen-derived lipid antigen. Proinflammatory signals activated during virus infection can activate iNKT cells through enhanced CD1d-dependent endogenous lipid presentation (31). In humans, a deficiency of NKT cells has been shown to be associated with severe and fatal herpesvirus infections (32). One immune evasion strategy of HSV is to downregulate the expression of CD1d on the surface of infected dendritic cells and monocytes (33, 34). HSV-1 infection in iNKT knockout (KO) mouse models demonstrated that these cells contribute to virus and disease control (32). Functionally polarized subsets of iNKT cells, iNKT1, iNKT2, and iNKT17, are generated in the thymus and secrete Th1-, Th2-, and Th17-like cytokines, respectively (35–39). The iNKT subsets are similar to MHC-restricted CD4$^+$ T cell subsets and share the same transcription factors that regulate their function (40–42). Three distinct thymic subsets have been identified based on their phenotype and the cytokines that they produce, including PLZF^{lo}, T-bet$^+$ (iNKT1), PLZF^{hi} GATA-3^{hi} (iNKT2), and PLZF^{int} RORγt$^+$ (promyelocytic leukemia zinc finger, retinoic acid-related orphan receptor gT) (iNKT17) (35–39). However, the role of the three major iNKT cell subsets, iNKT1, iNKT2, and iNKT17, in herpesvirus immunity remains to be fully elucidated. It is also not clear how iNKT cells affect antiviral responses and disease in these models. In this study, we examined the frequency and function of the three major iNKT cell subsets (i.e., iNKT1, iNKT2, and iNKT17) during early ocular herpesvirus infection in the corneas of HSV-1-infected asymptomatic (ASYMP) and symptomatic (SYMP) mice.

NKT cells are restricted by MHC class I-like CD1 molecules expressed on APCs, and because the CD1 molecule is also required for the development of CD1d-dependent NKT cells, CD1-deficient mice selectively lack CD1d-dependent NKT cells, with a KO of the *Cd1d1*/*Cd1d2* locus resulting in a lack of iNKT cells (32). Using CD1d KO mice, we analyzed if these cytokines secreted by iNKT cells play a role in ocular herpes. Both iNKT cells and DCs are programmed to migrate to inflamed peripheral tissue (43). In this study, we examined the molecular mechanisms contributing to infection and disease in

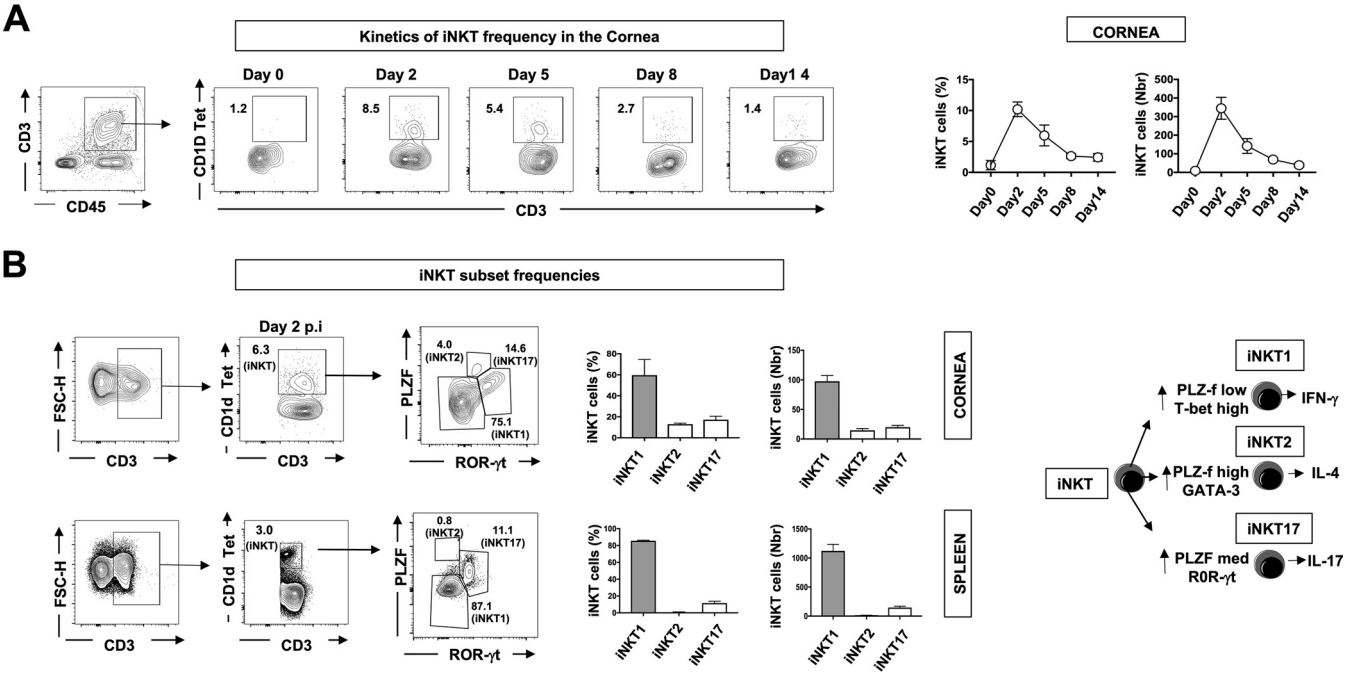

FIG 1 Kinetics of the frequencies of iNKT cell subsets in the corneas of CD1d KO mice following ocular herpetic infection. C57BL/6 ($n = 10$) mice were ocularly infected with HSV-1 (2×10^5 PFU/eye of the McKrae strain). Corneas were harvested at days 0, 2, 5, 8, and 14 postinfection (p.i.). Corneal single-cell suspensions were stained with mAbs specific for CD3 and CD1d Tet (iNKT cells), T-bet, GATA-3, and RORγt (iNKT1, iNKT2, and iNKT17 cell subsets) and analyzed by FACS staining. (A) Kinetics of iNKT frequencies in HSV-1-infected corneas. (Left) Representative contour plots of the frequencies of iNKT cells ($CD3^+$ CD1d Tet^+) detected in corneas of HSV-1-infected B6 mice at days 0, 2, 5, 8, and 14 p.i. (Right) Average frequencies of $CD3^+$ CD1d Tet^+ iNKT cells in corneas of HSV-1-infected B6 mice. (B) Frequencies of iNKT cell subsets (iNKT1, iNKT2, and iNKT17) detected in HSV-1-infected corneas on day 2 postinfection. (Left) Representative contour plots of the three major iNKT cell subsets detected in the corneas and spleens of HSV-1-infected B6 mice at day 2 p.i. (Middle) Average frequencies of iNKT1, iNKT2, and iNKT17 subsets in corneas and spleens of 10 HSV-1-infected B6 mice at day 2 p.i. Statistical analysis was performed using Student's *t* test. Nbr, number. (Right) Illustration of the phenotype and cytokine production of the iNKT1, iNKT2, and iNKT17 subsets.

the CD1d KO mouse model and report that the iNKT cell lineage is associated with protective immune responses during acute ocular HSV-1 infection in mice.

We report that early during acute ocular herpesvirus infection, the IFN-γ-producing $PLZF^{lo}ROR\gamma t^{lo}$ iNKT1 cell subset constitutes a major innate immune cell population that infiltrates the HSV-1-infected corneal tissue and contributes to the clearance of ocular herpesvirus infection and protection from cornea herpetic disease.

RESULTS

Increased frequency of the iNKT1 subset in the cornea early following ocular HSV-1 infection. We first studied iNKT cell frequencies in the corneas of C57BL/6 (B6) mice ($n = 10$) 0, 2, 5, 8, and 14 days following ocular HSV-1 infection with the laboratory HSV-1 strain McKrae at 2×10^5 PFU/eye. iNKT cells infiltrating the cornea were stained with monoclonal antibodies (mAbs) specific for mouse CD3, iNKT (CD1d tetramer [Tet]). There were significant increases in the percentage and number of iNKT cells infiltrating the infected cornea as early as day 2 following ocular HSV-1 infection (Fig. 1A). The average percentages of iNKT cells detected in the infected cornea at days 0, 2, 5, 8, and 14 postinfection (p.i.) were 1.2%, 8.5%, 5.4%, 2.7%, and 1.4% of the total CD3 cells, respectively. The frequency of iNKT cells infiltrating the cornea following ocular HSV-1 infection then gradually decreased to reach the postinfection level. The average numbers of iNKT cells detected in infected corneas at days 0, 2, 5, 8, and 14 were 30, 345, 142, 69, and 39 iNKT cells, respectively.

To determine the frequencies of the three major iNKT cell subsets, iNKT1, iNKT2, and iNKT17, in HSV-1-infected corneas, B6 mice were either infected with the HSV-1 laboratory strain McKrae at 2×10^5 PFU/eye ($n = 10$) or mock infected ($n = 10$). The corneas and spleens were harvested at 2 days postinfection, a time point when the peak of iNKT cell cellularity was reached in the cornea. The cornea and spleen cell

suspensions were then stained with mAbs specific for mouse CD3, iNKT (CD1d Tet); PLZF; and RORγt and analyzed by fluorescence-activated cell sorter (FACS) staining. Among the total $CD3^+$ $CD1d^+$ Tet^+ iNKT cell population, there was a significant increase in the frequency of the iNKT1 cell subset, compared to the iNKT2 and iNKT17 subsets (Fig. 1B). Specifically, in the corneas of 10 mice, the average frequency of the iNKT1 subset was 59.3%, and the iNKT17 subset represented 17.2%, while the iNKT2 subset represented only 9.8% (Fig. 1B, top). In the spleen (control), the percentage of iNKT cells was at a low average of 2.3% of the total CD3 cells. Spleen-derived iNKT cells had predominantly iNKT1 subsets (85.6% of iNKT cells), compared to low percentages of the iNKT2 and iNKT17 subsets (Fig. 1B, bottom).

Altogether, these results demonstrate that (i) there was an increased frequency of iNKT cells in the cornea early following ocular HSV-1 infection of B6 mice and (ii) $CD3^+$ $CD1d^+$ Tet^+ T-bet^+ $PLZF^{lo}ROR\gamma t^{lo}$ iNKT1 cells represent the major iNKT cell subset infiltrating the corneas of B6 mice early following ocular herpesvirus infection.

High frequency of the functional iNKT1 cell subset in the corneas of HSV-1-infected B6 mice is associated with asymptomatic ocular herpes. To further understand the role of the three major iNKT cell subsets (i.e., iNKT1, iNKT2, and iNKT17 cells) in protective innate immunity against corneal herpetic infection and disease, B6 mice were infected ocularly with HSV-1. On day 8 p.i., infected B6 mice were divided into symptomatic (SYMP) and asymptomatic (ASYMP) groups based on the severity of corneal herpes symptoms, as detailed in Materials and Methods. The frequencies and functions of the three major iNKT cell subsets were then compared on day 8 p.i. in SYMP and ASYMP mice. Single-cell suspensions of corneas obtained from infected mice at day 8 p.i. were stained with mAbs specific for CD3, iNKT (CD1d Tet); PLZF; and RORγt and analyzed by FACS staining. Early on, at 2 days postinfection, we detected significantly higher frequencies of iNKT1 cells in the corneas of HSV-1 infected ASYMP than in SYMP mice ($P < 0.05$) (Fig. 2A). Significantly higher percentages of iNKT cells ($CD3^+$ CD1d Tet^+) were detected in the corneas of HSV-1-infected ASYMP than in SYMP mice, as shown in representative contour plots (Fig. 2A, top) and by the average frequencies of $CD3^+$ CD1d Tet^+ iNKT cells (Fig. 2A, bottom). Specifically, there was an increased percentage (4.1% versus 1.4%) as well as an increased number (80 versus 24) of iNKT cells in single corneas of ASYMP mice compared to SYMP mice. In contrast, similar frequencies of iNKT cells were seen in the spleens (control compartment) (1.8% versus 1.6%) of the same SYMP and ASYMP mice (Fig. 2A, right).

Moreover, the iNKT cell subsets (iNKT1, iNKT2, and iNKT17) in the total iNKT ($CD3^+$ CD1d Tet^+) gated population in corneas at day 8 p.i. demonstrated a statistically significant increase in the percentage of the iNKT1 subset (49.4% versus 29.2%; $P < 0.05$) in SYMP and ASYMP mice, respectively (Fig. 2B). The function of cornea-derived iNKT cells was also greater in ASYMP than in SYMP mice. Specifically, there was a significant increase in the frequency of IFN-γ-producing iNKT cells in the corneas of ASYMP compared to the corneas of SYMP mice (44.8% versus 14.5%; $P = 0.05$) (Fig. 2C), further supporting the association of the functional iNKT1 cell subset with asymptomatic ocular herpes. In contrast, ASYMP mice showed a trend toward decreased IL-4 expression (24.1% versus 37.5%) compared to SYMP mice, supporting a lesser role for the functional iNKT2 cell subset in asymptomatic ocular herpes. There was no significant difference in the frequencies of IL-17-expressing iNKT17 cells in the corneas of SYMP compared to ASYMP mice ($P > 0.05$).

Altogether, these results indicate that (i) iNKT cells are major players in protective innate immunity during early ocular herpesvirus infection and (ii) the iNKT1 cell subset, but neither the iNKT2 nor the iNKT17 cell subset, plays a major role in protection from symptomatic corneal herpes.

CD1d KO mice, with iNKT cell deficiency, are more susceptible to HSV-1 ocular infection and disease. To better understand the role of cornea-resident iNKT cells in protection from ocular herpetic infection and disease, CD1d KO mice and wild-type (WT) B6 mice ($n = 10$) were similarly infected ocularly with 2×10^5 PFU/eye of HSV-1 (McKrae strain). Single-cell suspensions of the corneas, spleens, and livers (control)

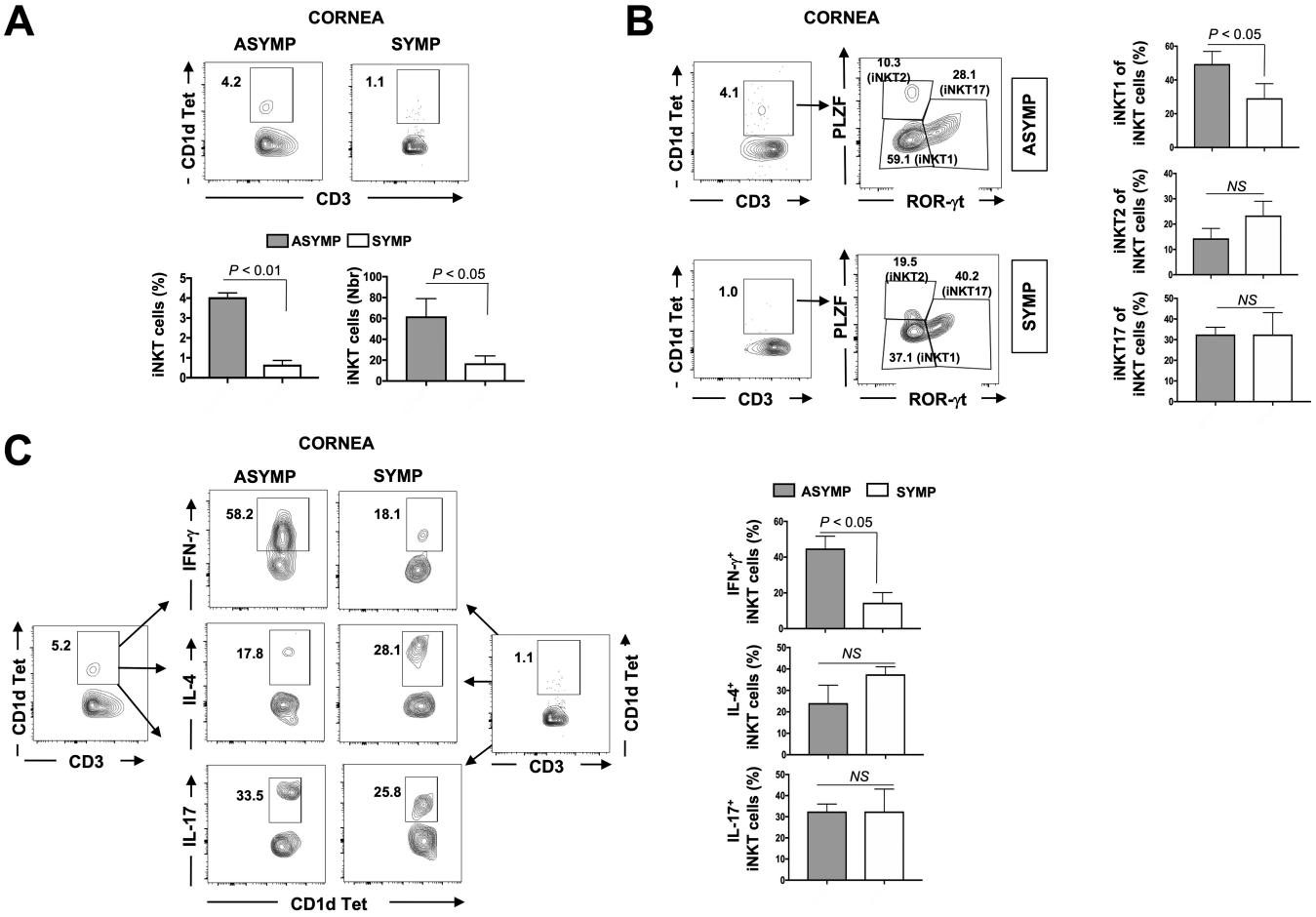

FIG 2 Frequencies and functions of the three major iNKT cell subsets in the corneas of HSV-1-infected symptomatic and asymptomatic mice. C57BL/6 ($n = 10$) mice were ocularly infected with HSV-1 (2×10^5 PFU/eye of the McKrae strain). At day 8 p.i., mice were separated into symptomatic (SYMP) and asymptomatic (ASYMP) groups based on the severity of ocular herpes disease, as detailed in Materials and Methods. Single-cell suspensions of corneas obtained from SYMP and ASYMP groups were stained with mAbs specific for CD3 and CD1d Tet (iNKT cells), T-bet, GATA-3, and RORγt (iNKT1, iNKT2, and iNKT17 cell subsets) and analyzed by FACS analysis. (A, top) Representative contour plots of the frequencies of iNKT cells ($CD3^+$ $CD1d\ Tet^+$) detected in corneas of HSV-1-infected SYMP and ASYMP B6 mice. (Bottom) Average frequencies of $CD3^+$ $CD1d\ Tet^+$ iNKT cells in the corneas of HSV-1-infected SYMP and ASYMP B6 mice. (B, left) Representative contour plots of the frequencies of iNKT cell subsets (iNKT1, iNKT2, and iNKT17) detected in corneas of 10 HSV-1-infected SYMP and ASYMP B6 mice. (Right) Graphs showing average frequencies of NKT1, NKT2, and NKT17 subsets in asymptomatic and symptomatic mice. (C) Function of iNKT cells from the corneas of HSV-1-infected SYMP and ASYMP B6 mice. Single-cell suspensions of corneas obtained from HSV-1-infected SYMP and ASYMP B6 mice were stimulated overnight with heat-inactivated HSV-1 and stained with mAbs specific for CD3, iNKT (CD1d Tet), IFN-γ, and IL-4. (Left) Representative contour plots of IFN-γ and IL-4 expression by iNKT cells from corneas of HSV-1-infected SYMP and ASYMP B6 mice. (Right) Average frequencies of $CD3^+$ $CD1d\ Tet^+$ iNKT cells in the corneas of HSV-1-infected SYMP (white bars) and ASYMP B6 mice. Statistical analysis was performed using Student's *t* test. NS, not significant.

obtained from CD1d KO mice at day 8 p.i. were stained with mAbs specific for CD3, iNKT (CD1d Tet), and analyzed by FACS staining, as described below. As expected, the percentage of iNKT cells was significantly lower in the corneas (0.15% versus 1.2%), spleens (0.09% versus 1.4%), and livers (1.0% versus 15.6%) of CD1d KO mice than in WT mice ($P < 0.05$) (Fig. 3A). iNKT cells were mostly localized in the stroma of the cornea of protected B6 mice (Fig. 3B). As shown in Fig. 3C, significantly higher virus titers were detected in ocular swabs of CD1d KO mice than in WT mice, collected at days 2, 5, and 7 p.i. (Fig. 3C, left). Specifically, on days 2, 5, and 7 p.i., we detected 8,705, 105,651 and 267 PFU/ml from eye swabs of CD1d KO mice, compared to only 8,203, 6,631, and 71 PFU/ml from eye swabs of WT B6 mice ($P < 0.05$). Similarly, up to 14 days p.i., there was significantly less survival of CD1d KO mice than of WT mice. Specifically, only 70% of mice survived HSV-1 infection with 2×10^5 PFU/eye of HSV-1 (McKrae strain), compared to 90% of WT mice (Fig. 3C). Mice were scored for ocular herpetic disease at days 2, 5, 7, 10, and 14 p.i., including the severity of pathological symptoms of keratitis and blepharitis, as detailed in Materials and Methods. As shown in Fig. 3D (bottom), there

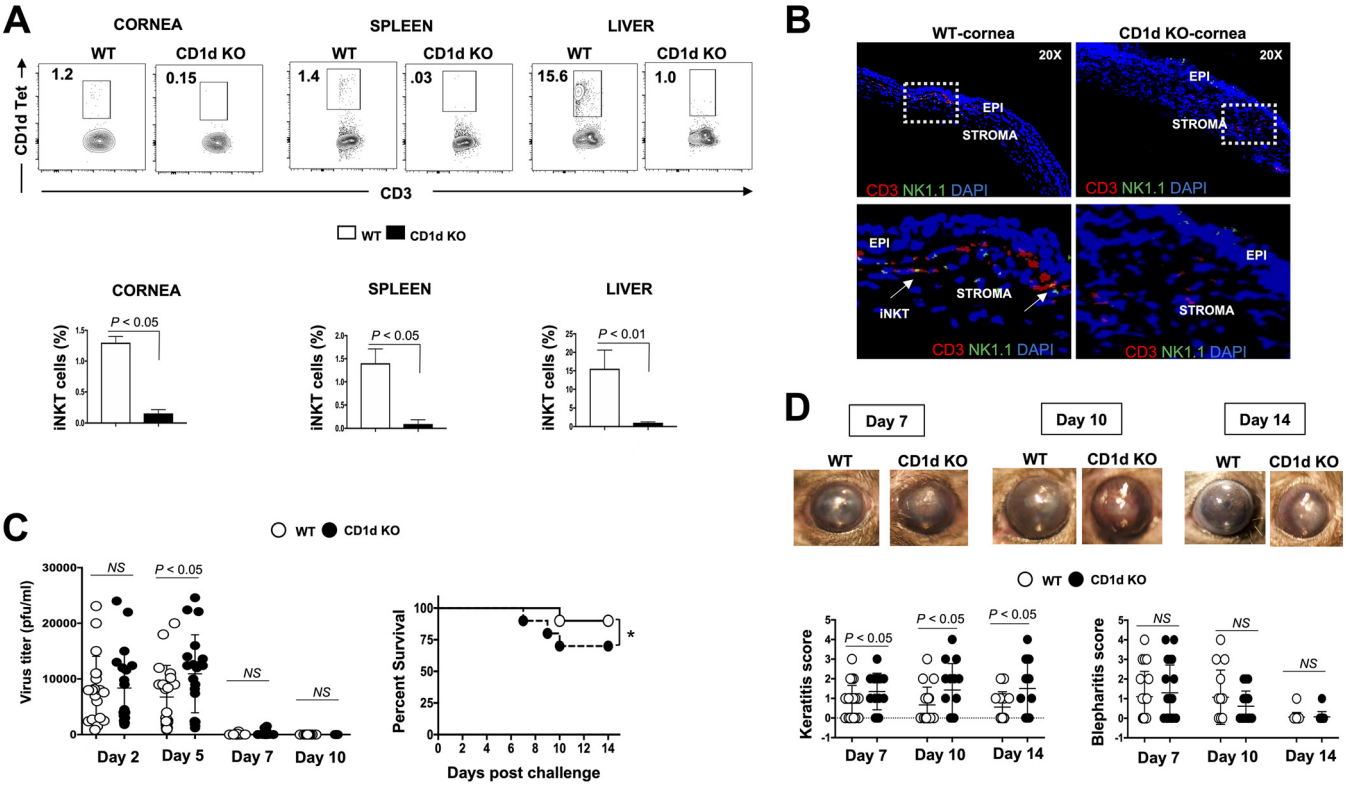

FIG 3 Ocular herpesvirus infection and disease in CD1d knockout mice lacking iNKT cells. CD1d knockout (KO) mice and wild-type (WT) B6 mice ($n = 10$) were ocularly infected with HSV-1 (2×10^5 PFU/eye of the McKrae strain). Single-cell suspensions of corneas, spleens, and livers were obtained from infected mice at day 8 p.i.; stained with mAbs specific for CD3 and CD1d Tet (iNKT cells), T-bet, GATA-3, and RORγt (iNKT1, iNKT2, and iNKT17 cell subsets); and analyzed by FACS staining. (A, top) Representative contour plots of the frequencies of iNKT cells ($CD3^+$ CD1d Tet^+) detected in corneas of HSV-1-infected CD1d KO and WT mice. (Bottom) Average frequencies of $CD3^+$ CD1d Tet^+ iNKT cells in the corneas of HSV-1-infected CD1d KO and WT mice. (B) Localization of NK1.1 cells in the corneas of CD1d KO and WT mice infected with HSV-1 at day 14 p.i. stained with CD3 and NK1.1 (arrows). EPI, epithelium. (C, left) Virus titers in HSV-1-infected CD1d KO and WT mice. Virus particles were measured by a plaque assay in eye swabs collected at days 2, 5, 7, and 10 p.i. Data are expressed as the mean PFU per milliliter ± standard errors of the means (SEM). (Right) Survival of HSV-1-infected CD1d KO and WT B6 mice. *, $P < 0.05$. (D, top) Representative eye pictures showing corneal herpetic disease (i.e., keratitis and blepharitis) in HSV-1-infected CD1d KO and WT B6 mice scored at days 7, 10, and 14 p.i. Stromal keratitis was scored as follows: 0 for no disease, 1 for cloudiness with some iris detail visible, 2 for obscured iris detail, 3 for totally opaque cornea, and 4 for cornea perforation. Blepharitis was scored as follows: 0 for no disease, 1 for puffy eyelids, 2 for puffy eyelids with some crusting, 3 for eye swollen shut with severe crusting, and 4 for eye completely swollen shut. (Bottom) Average corneal herpetic disease (i.e., keratitis and blepharitis) scores from 10 HSV-1-infected CD1d KO and WT mice on days 7, 10, and 14 p.i.

were significant increases in keratitis scores of CD1d KO mice compared to WT mice at day 7 (1.35 versus 0.75 for KO versus WT mice), day 10 (1.4 versus 0.6), and day 14 (1.5 versus 0.5).

Altogether, these results (i) indicate that a lack of iNKT cells in symptomatic CD1d KO mice is associated with increased HSV-1 ocular infection and disease and decreased survival and (ii) confirm the role of iNKT cells in early protection from corneal herpesvirus infection and disease in asymptomatic WT mice.

Downregulation of the IFN-γ pathway in HSV-1-infected corneas of CD1d KO mice is associated with symptomatic corneal herpetic disease. iNKT cells, which appear frequently in HSV-1-infected corneas, are known to rapidly secrete many cytokines, including IFN-γ, upon activation (12, 24, 40, 44). We therefore next compared the activation levels of the IFN-γ pathway and the amounts of a panel of 16 cytokines produced in the corneas of CD1d KO versus WT mice. Age- and gender-matched CD1d KO mice (which lack iNKT cells) and WT B6 mice ($n = 10$) were infected ocularly with 2×10^5 PFU/eye of HSV-1 (strain McKrae). HSV-1-infected corneas were harvested at days 2 and 5 p.i. and homogenized, and lysates were prepared for Western blot assays (Fig. 4A). Significant reductions in the levels of IFN-γ were detected in the corneas of CD1d KO mice compared to WT mice ($P < 0.01$) (Fig. 4A, top). To investigate the potential molecular mechanisms that subsequently follow the activation of the IFN-γ

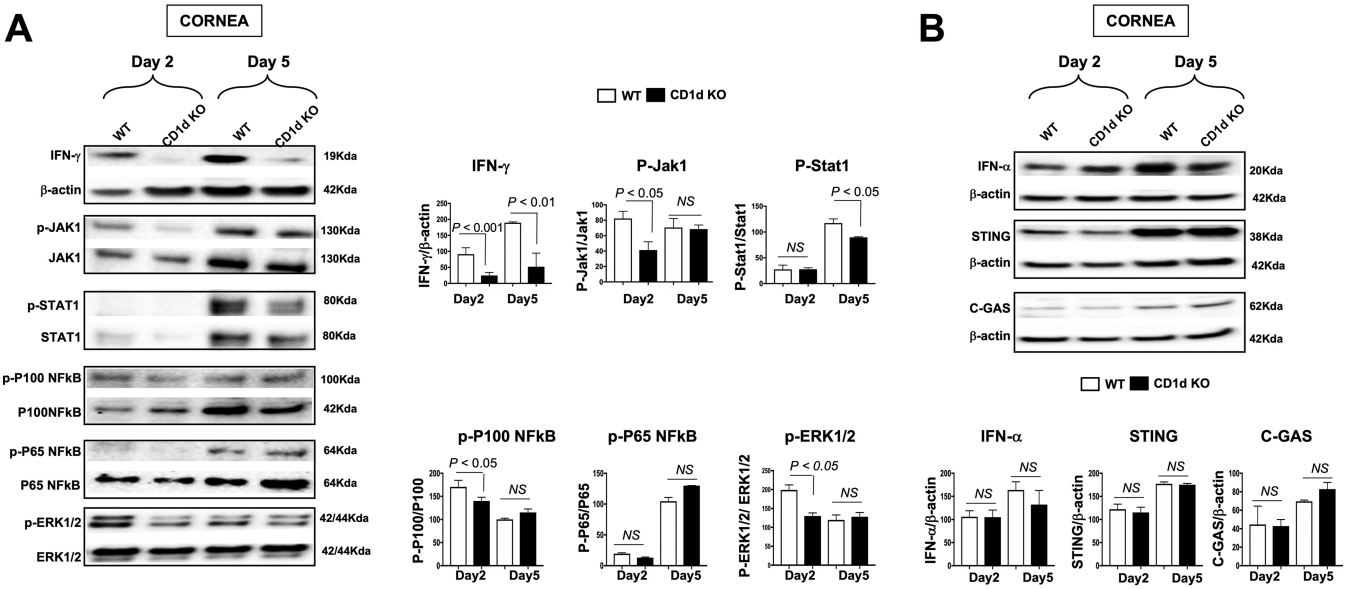

FIG 4 Activation of the IFN-γ pathway in CD1d KO and WT mice following ocular herpetic infection. CD1d KO mice and WT B6 mice ($n = 10$) were ocularly infected with HSV-1 (2×10^5 PFU/eye of the McKrae strain). Corneas were harvested at days 2 and 5 p.i., and total corneal lysates were used for Western blotting. (A, left) Immunoblots of whole corneal lysates were stained with mAbs specific for IFN-γ, Jak1, STAT1, p100 NF-κB, p65 NF-κB, and ERK1/2. (Right) corresponding mean percent relative intensities normalized to β-actin values from two sets of experiments. (B, top) Immunoblots of the whole corneal lysate were stained with mAbs specific for IFN-γ, STING, C-GAS, and β-actin. (Bottom) Corresponding mean percent relative intensities normalized to β-actin values from two sets of experiments.

pathway in HSV-1-infected cornea-resident iNKT cells, we compared the levels of activation of the JAK1, STAT1, p100 NF-κB, p65 NF-κB, and extracellular signal-regulated kinase 1/2 (ERK1/2) pathways in the corneas of CD1d KO versus WT mice at 2 and 5 days postinfection. As early as 2 days postinfection and concomitant with the reduction in the level of IFN-γ, we detected significant decreases in the activation levels of JAK1, STAT1, p100 NF-κB, and ERK1/2 in the corneal lysates of CD1d KO mice compared to WT mice ($P < 0.05$) (Fig. 4A). Subsequently, on day 5 postinfection, there were also significant decreases of both IFN-γ and STAT1 in the corneas of HSV-1-infected CD1d KO mice compared to the corneas of HSV-1-infected WT mice. However, on days 2 and 5 postinfection, no significant differences in the levels of p65 NF-κB and β-actin (control) were detected in the corneas of HSV-1-infected CD1d KO versus WT mice ($P > 0.05$) (Fig. 4A). Thus, IFN-γ and its downstream signaling molecules were downregulated in CD1d KO mice. However, the DNA-sensing pathway induced by herpesvirus infection that stimulates cGAS (cyclic GMP-AMP synthase), STING (cGAS stimulator of interferon genes), and the IFN-γ pathway was not altered in CD1d KO mice (Fig. 4B).

These results indicate that (i) the downregulation of the levels of IFN-γ and its downstream cascade pathways in HSV-1-infected corneas of CD1d KO mice is associated with symptomatic corneal herpetic disease and, in contrast, (ii) the upregulation of the levels of IFN-γ and its downstream cascade pathways in HSV-1-infected corneas of WT mice is associated with asymptomatic herpes.

Altered cytokine profile of IFN-γ, IL-6, and IL-12 in HSV-1-infected corneas of CD1d KO mice is associated with symptomatic corneal herpetic disease. We confirmed a significant decrease in level of IFN-γ in nonprotected corneas of CD1d KO mice compared to protected corneas of WT mice (35 pg/ml versus 19 pg/ml at day 2, and 230 pg/ml versus 110 pg/ml at day 5 p.i., respectively) (Fig. 5A) using a Luminex assay for 16 of the most well-known inflammatory cytokines, including IFN-γ, IL-1α, IL-1β, IL-2, IL-4, IL-5, IL-6, IL-10, IL-12p40, IL-12p70, IL-15, IL-17, IP-10 (IFN-γ inducible protein 10) macrophage colony-stimulating factor (M-CSF), and tumor necrosis factor alpha (TNF-α). In addition to IFN-γ, the secretion of IL-6 was increased in the corneas of CD1d KO mice compared to the corneas of WT mice at day 2 p.i.

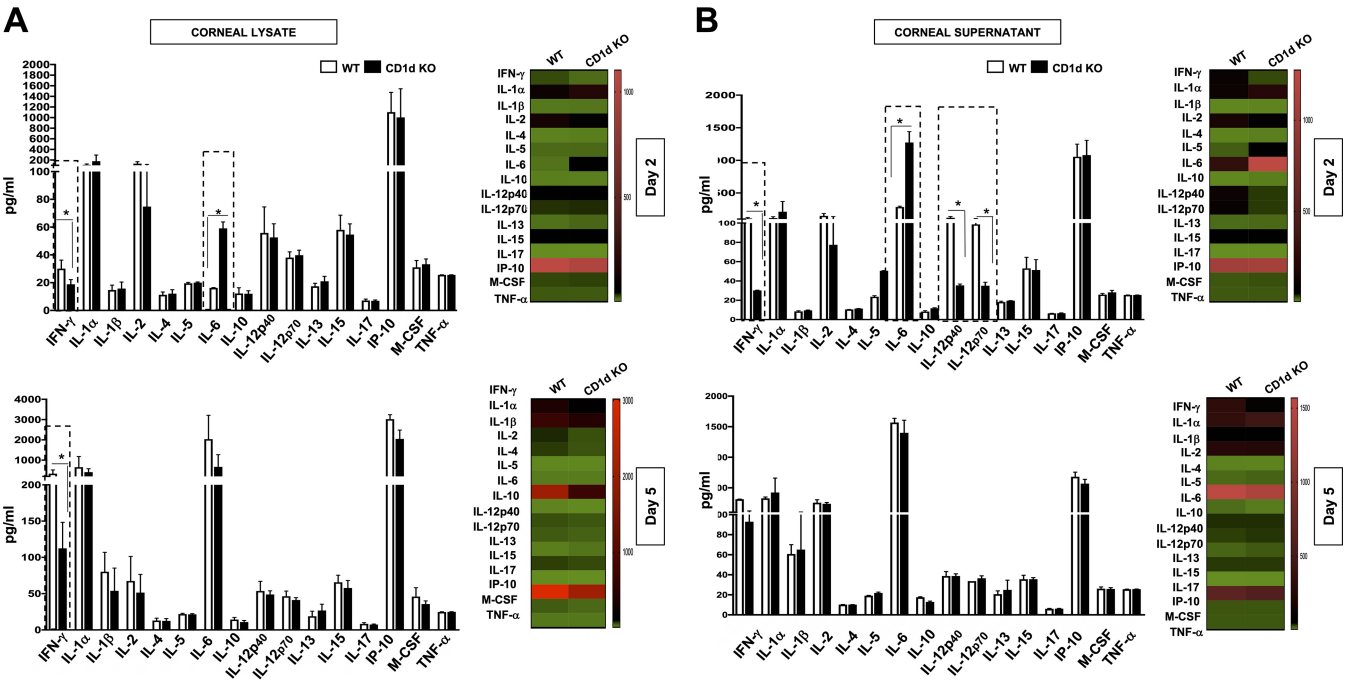

FIG 5 Cytokine profiles in corneas of CD1d KO and WT mice following ocular herpetic infection. (A) CD1d KO mice and WT B6 mice ($n = 10$) were ocularly infected with HSV-1 (2×10^5 PFU/eye of the McKrae strain). Corneas were harvested at days 2 and 5 p.i., and total corneal lysates were used for a Luminex cytokine assay. Uninfected cells were used as negative controls. (Left) Levels of IFN-γ, IL-1α, IL-1β, IL-2, IL-4, IL-5, IL-6, IL-10, IL-12p40, IL-12p70, IL-15, IL-17, IP-10, M-CSF, and TNF-α detected using a Luminex assay in the corneal extracts of HSV-1-infected mice at day 2 (top) and day 5 (bottom) p.i. (Right) Corresponding heat map of the cytokine profile. (B) At days 2 and 5 p.i., corneal cells from WT and CD1d KO mice were isolated and stimulated with heat-inactivated HSV-1 McKrae. The corneal cell culture supernatant was used for a Luminex cytokine assay. (Left) Levels of IFN-γ, IL-1α, IL-1β, IL-2, IL-4, IL-5, IL-6, IL-10, IL-12p40, IL-12p70, IL-15, IL-17, IP-10, M-CSF, and TNF-α detected using a Luminex assay in the corneal cell supernatants of HSV-1-infected mice at day 2 (top) and day 5 (bottom) p.i. (Right) Corresponding heat map of cytokines. Statistical analysis was performed using Student's *t* test.

Corneal cells from symptomatic CD1d KO mice stimulated with heat-inactivated HSV-1 McKrae showed a significant decrease in the level of IFN-γ compared to corneal cells from asymptomatic WT mice (i.e., 109 pg/ml versus 30 pg/ml on day 2 postinfection, respectively) (Fig. 5B). In contrast, on day 2 postinfection, we detected a decrease in the level of IL-6 in the corneas of asymptomatic WT mice compared to the corneas of symptomatic CD1d KO mice (i.e., 284 versus 1,274 pg/ml) (Fig. 5B). Also, symptomatic CD1d KO mouse corneas showed decreased levels of DC (dendritic cell)-secreted cytokines such as IL-12p40 (120 versus 35 pg/ml) and IL-12p70 (98.6 versus 35 pg/ml) upon stimulation.

These results indicate that (i) increased production of IL-6, as early as 2 days postinfection, was associated with severe symptomatic inflammatory ocular herpetic disease and (ii) increased production of IFN-γ and IL-12 was associated with asymptomatic corneal herpetic infection.

Decreased frequency of activated DCs in the corneas of HSV-1-infected CD1d KO mice. To further investigate the cellular mechanism underlying the severe cornea herpes observed in CD1d KO mice, we determined the frequency and activation of B cells and DCs, two innate immune cell types known to interact with iNKT cells (45–48) (Fig. 6A). Age- and gender-matched CD1d KO mice and WT B6 mice ($n = 10$) were similarly infected ocularly with 2×10^5 PFU/eye of HSV-1 (strain McKrae). Single-cell suspensions of the corneas, spleens, and livers (control) obtained from CD1d KO mice at days 2 and 5 p.i. were stained with mAbs specific for mouse CD1d, B220, CD11b, CD11c, and CD3, iNKT (CD1d Tet), and analyzed using FACS staining, as described above.

Two and five days after ocular HSV-1 infection, there was a significant decrease in the frequency of DCs detected in the corneas of CD1d KO mice compared to WT mice. Specifically, on day 2 p.i., there were 12.5% versus 5.9% DCs, and on day 5 p.i.,

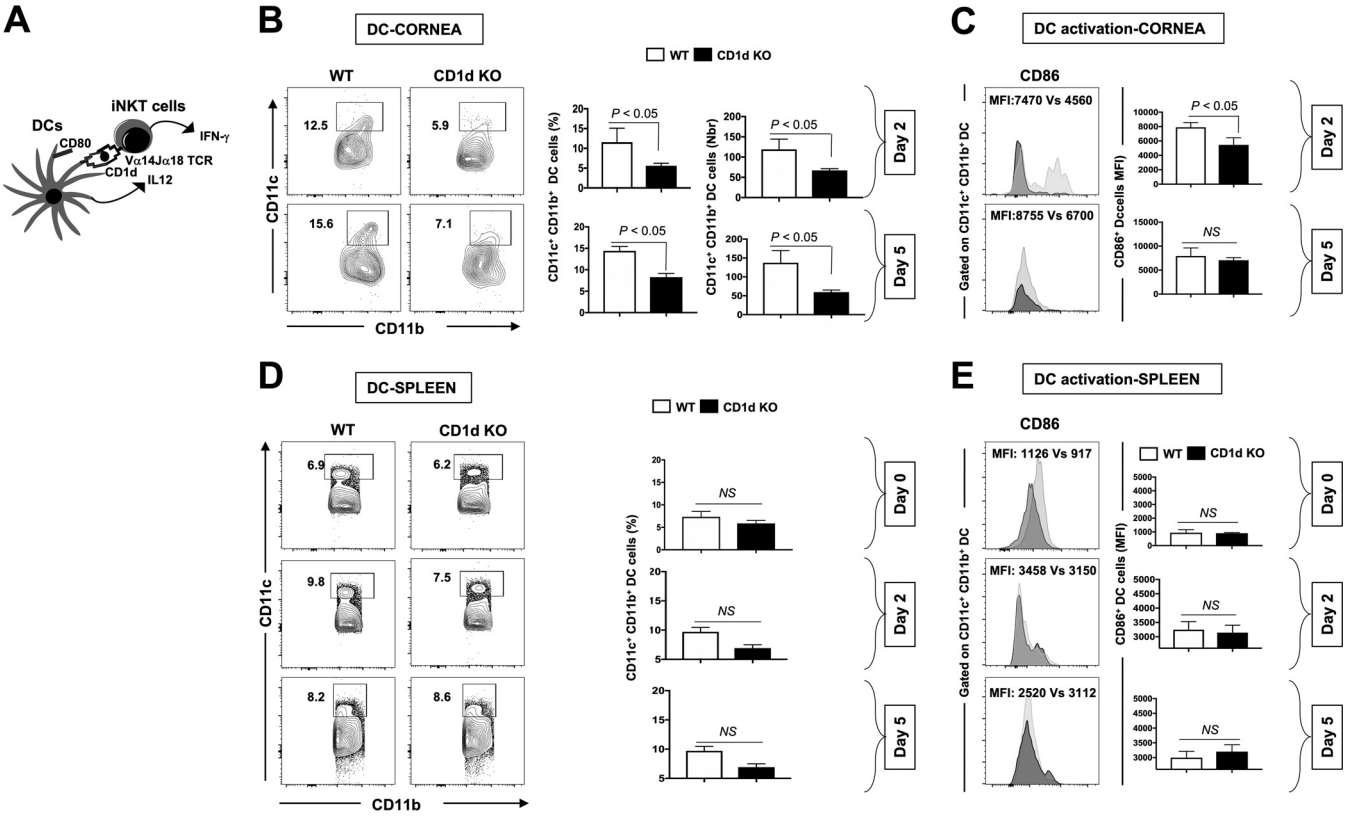

FIG 6 DC activation in CD1d KO mice during ocular herpetic infection. CD1d KO mice and WT B6 mice ($n = 10$) were ocularly infected with HSV-1 (2×10^5 PFU/eye of the McKrae strain). Corneas were harvested at days 2 and 5 p.i., and single-cell suspensions were stained with Abs specific for murine CD45, CD11b, CD11c, F4/80, MHC class II, and CD86 and analyzed using FACS staining. Uninfected cells were used as negative controls. (A) Illustration of iNKT-DC interactions in the cornea. IL-12 is secreted by DCs, which in turn stimulates IFN-γ production by the neighboring iNKT1 cell subset. (B, left) Representative contour plots of the frequencies of DCs ($CD45^+$ $CD11b^+$ $CD11c^+$ $F4/80^-$) detected at days 2 and 5 p.i. in the corneas of HSV-1-infected CD1d KO and WT mice. (Right) Average frequencies of DCs in the corneas of HSV-1-infected CD1d KO and WT mice. (C, left) Representative histograms showing CD80 upregulation on gated $CD11c^+$ $CD11b^+$ DCs from the corneas of HSV-1-infected CD1d KO and WT mice on days 2 and 5 p.i. (Right) Average MFIs of CD86 in corneal DCs at days 2 and 5 p.i. (D, left) Representative contour plots of the frequencies of DCs detected at days 2 and 5 p.i. in the spleens (control) of HSV-1-infected CD1d KO and WT mice. (Right) Average frequencies of DCs in the spleens of HSV-1-infected CD1d KO and WT mice. (E, left) Representative histograms showing CD80 upregulation on gated $CD11c^+$ $CD11b^+$ DCs from the spleens of HSV-1-infected CD1d KO and WT mice at days 2 and 5 p.i. (Right) Average MFIs of CD86 in spleen-derived DCs at days 0, 2, and 5 p.i. Statistical analysis was performed using Student's *t* test.

there were 15.6% versus 7.1% DCs, in HSV-1-infected corneas of CD1d KO mice compared to corneas of WT mice (Fig. 6B). There was a significant decrease in the expression of the CD86 activation marker detected on DCs from the corneas of CD1d KO mice compared to the corneas of WT mice (mean fluorescence intensity [MFI], 7,987 versus 5,457) on day 2 p.i. (Fig. 6C). There was no significant difference observed in either the activation or the expression of CD86 on gated DCs in the corneas of B6 and CD1d KO mice infected with McKrae at day 5 p.i. (MFI, 7,935 versus 7,054). To determine whether the effect on the activation of DCs was specific to the cornea (the site of acute infection), we studied the frequency and activation of DCs in other compartments, such as the spleen and liver (controls). No differences were detected in the frequency (Fig. 6D) and activation (Fig. 6E) of DCs ($CD45^+$ $CD11b^+$ $CD11c^+$ $F4/80^-$) derived from the spleens at day 0 (MFI, 942 versus 902), day 2 p.i. (MFI, 3,256 versus 3,207), and day 5 p.i. (MFI, 3,105 versus 3,376) between the CD1d KO and B6 mice.

Being a professional antigen-presenting cell type, DCs express CD1d that can present lipid antigens to NKT cells. In CD1d KO mice, as expected, there was a significant downregulation of the expression of CD1d on both B cells and DCs compared to WT mice (see Fig. S1 in the supplemental material). Also, as expected, the frequency of NKT2 cells ($NK1.1^+$ and $CD3^+$) was significantly lower in the corneas of symptomatic CD1d KO mice than in the corneas of asymptomatic WT mice ($P < 0.05$)

(Fig. S1). A low frequency of the CD1d-independent NKT-like cell subset ($NK1.1^+$ and $CD3^+$) was also present in the corneas of symptomatic CD1d KO mice.

These results demonstrate (i) a decreased frequency and reduced activation of DCs in the corneas of CD1d KO mice versus WT mice and (ii) that these differences in the frequency and activation of DCs are specific to infected corneas.

DISCUSSION

Invariant NKT (iNKT) cells are among the innate immune cells that respond quickly to invading viral pathogens during early phases of infections (reviewed in references 31 and 49). In the present study, we discovered that during acute ocular herpesvirus infection, the IFN-γ-producing $PLZF^{lo}ROR\gamma t^{lo}$ iNKT1 cell subset constitutes a major innate immune cell population that infiltrates the HSV-1-infected cornea and contributes to the clearance of ocular herpesvirus infection and to protection from cornea herpetic disease.

Three distinct major subsets of iNKT cells were identified based on their phenotype and cytokine profile: (i) the iNKT1 subset, which is $PLZF^{lo}$ and T-bet^+ (iNKT1) and produces mainly IFN-γ; (ii) the iNKT2 subset, which is $PLZF^{hi}$ and GATA-3^{hi} and produces mainly IL-4 (these $PLZF^{hi}$ GATA-3^{hi} iNKT2 cells consist of a mixed population of cells that are not fully differentiated [39, 50]); and (iii) the iNKT17 subset, which is $PLZF^{int}$ and $ROR\gamma t^+$ and produces mainly IL-17 (35, 51, 52). Our results show both quantitative and qualitative differences in the iNKT cell subsets between asymptomatic and symptomatic mice. We identified a major proportion of the IFN-γ-producing $PLZF^{lo}ROR\gamma t^{lo}$ iNKT1 cell subset infiltrating the cornea early, within the first 7 days of ocular HSV-1 infection. In contrast, the iNKT2 and iNKT17 subsets constitute only a minority iNKT cell proportion in HSV-1-infected corneas during the acute phase of infection. Moreover, we demonstrated that the high proportion of IFN-γ-producing $PLZF^{lo}ROR\gamma t^{lo}$ iNKT1 cells in HSV-1-infected corneas is associated with asymptomatic ocular herpes, suggesting their role in reducing virus replication with a-yet-to-be-determined mechanism. There was a significant increase in $PLZF^{lo}ROR\gamma t^{lo}$ iNKT1 cells in the corneas of HSV-1-infected "protected" asymptomatic B6 mice compared to the corneas of "nonprotected" B6 symptomatic mice. As early as 2 days postinfection, we detected a significant increase in the frequencies of the NKT1 subset in the corneas (59.6%) and spleens (85.6%) of HSV-1-infected WT mice. Although the frequency of the iNKT1 subset is slightly lower in the cornea than in the spleen, the enriched local NKT1 subset in the infected cornea likely plays a critical role in innate protection early during ocular HSV-1 infection. In addition, we demonstrated increased IFN-γ production by iNKT cells in protected asymptomatic B6 mice upon infection with HSV-1, suggesting a direct link between the amount of replicating virus and the local activation of iNKT cells. As expected, significantly lower frequencies of iNKT cells were detected in the corneas of HSV-1-infected CD1d KO mice than in the corneas of HSV-1-infected B6 WT mice. The background detected in the livers of CD1d KO mice was likely due to the specific mouse strain used and/or to nonspecific binding of CD1d tetramer antibodies (Abs). Moreover, we found that the absence of CD1d expression or iNKT cells modulates DC activation and function using CD1d KO mice. Invariant NKT cells have been reported to play various roles in virus infection, such as in the regulation of other cell subsets like NK cells, regulatory T cells, and B cells. However, besides the present study, there is no literature on the recently identified iNKT cell lineages (iNKT1, iNKT2, and iNK17) and their association with the protective immune response to ocular herpes.

In agreement with data from previous studies (53–56), we detected an increased frequency of iNKT cells in the corneas of HSV-1-infected B6 mice early during ocular herpesvirus infection. Although there was an increase in the frequency of IFN-γ-producing $PLZF^{lo}ROR\gamma t^{lo}$ iNKT1 cells in the corneas of HSV-1-infected asymptomatic mice, compared to the corneas of HSV-1-infected symptomatic mice, the causes of such an increased frequency of iNKT1 cells in protected asymptomatic corneas and the underlying protective cellular and molecular mechanisms by which iNKT cells

may directly or indirectly control HSV-1 infection and disease remain to be fully elucidated (7).

The factors that are responsible for this cornea inflammation during ocular herpesvirus infection are proinflammatory cytokines and chemokines (57, 58). Many of these factors have been defined for primary cornea herpetic disease (57, 58). One important feature of iNKT function is the rapid production of a vast array of cytokines, including IFN-γ, TNF-α, IL-2, IL-4, IL-5, IL-6, IL-10, IL-13, IL-17, and IL-21 (12, 24, 40, 44), and chemokines, including CXCR3 chemokines (59). A decline in these cytokines/chemokines due to the absence of iNKT cells in the corneas of HSV-1-infected CD1d KO mice would lead to an increase in virus replication and a worsening of corneal disease, suggesting a major role for cytokines/chemokines produced by iNKT cells during early ocular herpesvirus infection. We found increased IFN-γ production in the asymptomatic corneas of WT mice, suggesting the activation of IFN-γ-producing iNKT cells, compared to the symptomatic corneas of CD1d mice that lack iNKT cells. Interestingly, the level of the inflammatory cytokine IL-6 was increased in the corneas of HSV-1-infected CD1d mice, suggesting its involvement in the inflammatory corneal herpetic disease seen in these mice. However, no difference was detected in other cytokines, such as IL-2, IL-4, IL-5, IL-10, IL-13, IL-17, IL-21, IP-10, M-CSF, and TNF-α, in the corneas of HSV-1-infected WT versus HSV-1-infected CD1d KO mice.

Similar to data from previous reports (32, 60–68), we detected high levels of virus replication and severe herpetic disease in CD1d KO mice compared to WT mice. The missing iNKT cell-mediated protective mechanisms or disease-mediated mechanisms in CD1d KO mice would be caused by a lack of IFN-γ-producing PLZF^{lo}RORγt^{lo} iNKT1 cells, a cell population that is highly presented in the protected asymptomatic corneas of WT mice. Furthermore, unlike for the IFN-γ pathway, we found no difference in the IFN-γ and the cGAS-STING pathways in the corneas of CD1d KO mice versus WT mice, pointing a major role of IFN-γ in the observed protection. This possibly also suggests that, unlike the role of the IFN-γ pathway in controlling virus replication and disease, there was no apparent role for the IFN-γ pathway in protection from virus replication and herpetic disease. The inflammatory cytokine IFN-γ activates the mitogen-activated protein kinase (MAPK) (ERK1/2) and NF-κB signaling pathways by binding to the corresponding receptors (69, 70). We observed a decrease in the activation of both the p-ERK and NF-κB pathways, probably mediated through Jak1-Stat1, in CD1d KO mice during ocular herpesvirus infection, confirming the downregulation of the IFN-γ pathway that would provide protection from virus replication and disease. The major output of the MAPK and NF-κB signaling cascades downstream will be a proinflammatory response; hence, the activation of these pathways may indicate an early protective inflammatory response (5, 71–75). In addition, we demonstrated that IFN-γ is the major cytokine directly released, or indirectly upregulated, by iNKT cells in the cornea, compared to the 15 other cytokines studied. Moreover, the observed decrease in the frequency and activation of cornea-resident DCs suggests interregulation between DCs and iNKT cells, with a yet-to-be-determined mechanism, in the HSV-1-infected cornea.

In this study, we found that an increased level of the proinflammatory cytokine IL-6 in corneas, as early as 2 days postinfection, was associated with severe inflammatory ocular herpetic disease in symptomatic CD1d KO mice. This suggests a pathogenic role of IL-6 in HSV-1-infected symptomatic corneas, with a yet-to-be-determined immunopathological mechanism. IL-6 and the related family members IL-1, IL-8, IL-18, IL-33, and TNF-α (CXCL8) are the prototype cytokines associated with inflammatory responses to many infectious diseases (76–81). During early HSV-1 infection, IL-6 can be produced by many immune and nonimmune cells, including mononuclear phagocytes, DCs, endothelial cells, and fibroblasts, in the symptomatic cornea. In contrast, a lower level of IL-6 was detected in the asymptomatic corneas from WT B6 mice. This result is in agreement with a previous report of reduced neutrophil-attracting IL-6 and a reduced population of neutrophils in the corneas of HSV-1-infected asymptomatic mice, with no herpetic stromal keratitis (HSK) (81). Unlike IL-6, the level of IFN-γ was increased on days 2 and 5 postinfection in the asymptomatic corneas of WT B6 mice compared to the symp-

tomatic corneas of CD1d KO mice, suggesting a protective role of IFN-γ. IFN-γ is likely produced by the abundant iNKT1 cell subset detected in the asymptomatic corneas of WT B6 mice. Finally, on day 2 postinfection, we found an increase in the level of IL-12 in the asymptomatic corneas of WT B6 mice compared to the symptomatic corneas of CD1dKO mice, also suggesting a protective role of IL-12. Because the asymptomatic corneas of WT B6 mice also presented frequent DCs, it is likely that IL-12 was secreted locally by these frequent DCs, which in turn stimulated the neighboring abundant iNKT1 cells, also abundant in the asymptomatic cornea, to produce IFN-γ, a major factor that interferes with virus replication.

HSK is characterized by an inflammatory response that includes neutrophils, macrophages, NK cells, iNKT cells, and T cells (8–11, 57, 82). Although this study demonstrates the role of iNKT1 cells in early protection from primary corneal herpetic disease (acute HSK), their role in protection from recurrent HSK (rHSK) remains to be fully elucidated. In humans, differences in the numbers and functions of NK cells have been reported to affect the prognosis of recurrent herpetic stromal keratitis (83). However, the role of iNKT cells in protection from recurrent herpetic stromal keratitis in humans, or in animal models of recurrent herpes, has not been reported. We are currently comparing the roles of various iNKT cell subsets in protection from recurrent herpetic stromal keratitis in both symptomatic/asymptomatic humans and a UVB-induced recurrent herpes mouse model (84–86), and the results will be the subject of future reports. The CD1d KO mouse model used in this study lacks the lipid antigen-presenting molecule on various antigen-presenting cells (including B cells and DCs), as shown in Fig. S1 in the supplemental material. At this juncture, we do not know if a lack of CD1d contributes to symptomatic disease by any means.

In conclusion, the findings reported here suggest (i) an increase in the frequency of iNKT cells infiltrating the HSV-1-infected cornea early during infection; (ii) that cornea-resident IFN-γ-producing PLZF^{lo}RORγt^{lo} iNKT1 cells are major protective innate cells infiltrating the cornea during early acute corneal infection; (iii) an increase in the iNKT1 frequency is associated with decreases in virus replication and disease in corneas in asymptomatic B6 mice; (iv) a lack of iNKT cells in CD1d KO mice is associated with a profound decrease in local IFN-γ secretion in the cornea, which is subsequently associated with the downregulation of the MAPK (ERK1/2) and NF-κB signaling pathways; and (v) a reduced frequency of maturated DCs in the cornea during ocular herpesvirus infection may interregulate iNKT1 cell frequency and function, leading to severe corneal herpetic disease. Overall, to the best of our knowledge, we are the first group to report the high frequency of the IFN-γ-producing PLZF^{lo}RORγt^{lo} iNKT1 cell subset infiltrating the cornea early during HSV-1 infection and its association with asymptomatic ocular herpes.

MATERIALS AND METHODS

Virus propagation and titration. The HSV-1 laboratory strain McKrae was used throughout this study. For virus propagation, rabbit skin (59) cells (ATCC, Manassas, VA) were grown in Eagle minimum essential medium with Earle's salts and L-glutamine (Corning, Manassas, VA) supplemented with 10% fetal bovine serum (FBS) and 1% penicillin-streptomycin. HSV-1 was propagated in rabbit skin (RS) cells, as we described previously (87); purified by ultracentrifugation in a sucrose gradient; and titrated by a plaque assay. Uninfected cells were used as negative controls.

Mice. Animal studies were conducted with the approval of the Institutional Animal Care and Use Committee (IACUC) of the University of California, Irvine (approval no. 19-111) and conformed to the recommendations of the *Guide for the Care and Use of Laboratory Animals* of the U.S. National Institutes of Health (88). Female C57BL/6 (B6) WT and CD1d KO mouse breeder pairs (6 to 8 weeks of age) were purchased from the Jackson Laboratory (Bar Harbor, ME).

Ocular infection with HSV-1. Mice were infected with 5×10^5 PFU per eye of HSV-1 strain McKrae via eye drops in a total of 2 μl sterile phosphate-buffered saline (PBS) after corneal scarification (i.e., light scratches) in a crosshatched pattern (4 to 5 vertical and 4 to 5 horizontal scratches) with a 25-gauge needle. Mice were monitored daily for ocular herpesvirus infection and disease progression. To examine corneal inflammation and cloudiness, pictures were taken at several time points with a Nikon D7200 camera.

Ocular herpesvirus infection and disease monitoring and scoring in mice. Virus shedding was quantified in eye swabs collected at days 2, 5, 7, and 10 p.i. Eyes were swabbed using moist swabs and frozen at −80°C until titrated on RS cell monolayers, as described previously (87). Mice were scored on

days 2, 5, 7, 10, and 14 for pathological symptoms of keratitis and blepharitis after infection with the HSV-1 McKrae strain at 2×10^5 PFU/eye. Stromal keratitis was scored as follows: 0 for no disease, 1 for cloudiness with some iris detail visible, 2 for obscured iris detail, 3 for totally opaque cornea, and 4 for cornea perforation. Blepharitis was scored as follows: 0 for no disease, 1 for puffy eyelids, 2 for puffy eyelids with some crusting, 3 for eye swollen shut with severe crusting, and 4 for eye completely swollen shut. The graphs show the corresponding keratitis and blepharitis scores at days 7, 10, and 14 p.i. The average total score for each group was calculated by dividing the total score for each day by the total number of eyes in each group. HSV-1-infected mice were segregated into two groups: (i) the asymptomatic (ASYMP) group, with no recurrent corneal herpes disease (with severity of disease scored from 0 to 1 on a scale of 0 to 4), and (ii) the symptomatic (SYMP) group (with severe corneal herpetic disease with a score of 2 to 4 on a scale of 0 to 4).

Flow cytometry. Single-cell suspensions from the mouse corneas after collagenase treatment (15 mg/ml) for 1 h were used for fluorescence-activated cell sorter (FACS) staining. The following antibodies (all purchased from BD Biosciences, Franklin Lakes, NJ) were used: anti-mouse CD3 (clone 17A-2), CD45 (clone 30-F11), CD11c (clone HL3), CD11b (clone M1/70), F4/80 (clone BM8), T-bet (clone 04-46), GATA-3 (clone L50-823), RORγt (clone q31-378), CD80 (clone 16-10A1), HLA-DR (clone M5/114), and CD1d Tet specific for the mouse Vα14Jα18 TCR for iNKT cells (NIH tetramer core facility, Emory University, Atlanta, GA). For surface staining, mAbs against various cell markers were added to a total of 1×10^6 cells in PBS containing 1% FBS and 0.1% sodium azide (FACS buffer) and left for 45 min at 4°C. For intracellular/intranuclear staining, cells were first treated with Cytofix/Cytoperm (BD Biosciences) for 30 min. Upon washing with Perm/Wash buffer, mAbs were added to the cells, and the cells were incubated for 45 min on ice in the dark, washed with Perm/TF Wash and FACS buffers, and fixed in PBS containing 2% paraformaldehyde.

Immunohistochemistry. Mouse corneas were flash frozen in optimal cutting temperature (OCT) compound and sectioned at a 10-μm thickness for immunohistochemistry (IHC). Indirect immunofluorescence staining was performed by incubation with the primary antibody overnight, followed by the secondary antibody for 1 h at room temperature. The primary antibodies used were anti-mouse CD11c, CD3, and NK1.1 (BD Biosciences). Secondary antibodies included goat anti-mouse Cy5 antibody and goat anti-rabbit Cy3 antibody (all purchased from Jackson Immunoresearch, West Grove, PA). After 3 PBS washes, slides were mounted with Fluoromount-G with 4′,6-diamidino-2-phenylindole (DAPI) (Invitrogen, Carlsbad, CA). Images were captured on a BZ-X710 All-in-One fluorescence microscope (Keyence Corporation of America, Itasca, IL).

Western blotting. Corneas were dissected, homogenized in lysis buffer (radioimmunoprecipitation assay [RIPA] buffer supplemented with 1% protease inhibitor) and stored at −80°C for Western blot assays and enzyme-linked immunosorbent assays (ELISAs). Cell lysates were quantified, and 30 μg of protein was loaded onto SDS-PAGE (4 to 15%) gels for electrophoresis and then transferred to a polyvinylidene difluoride (PVDF) membrane (Merck Millipore, Burlington, MA). After blockade with 5% bovine serum albumin (BSA), the membranes were incubated with primary antibodies, including anti-mouse IFN-γ (clone 37895; R&D Systems, Minneapolis, MN), IFN-α (catalog no. PA5-86767; Invitrogen), phospho-NF-κB p65 (catalog no. 3033S; Cell Signaling Technology, Danvers, MA), NF-κB p65 (catalog no. 8242S; Cell Signaling Technology), phospho-NF-κB2 p100 (catalog no. 4810S; Cell Signaling Technology), NF-κB2 p100 (catalog no. 4882S; Cell Signaling Technology), phospho-p44/42 MAPK (catalog no. 9101; Cell Signaling Technology), p44/42 MAPK (catalog no. 9102; Cell Signaling Technology), and β-actin (Cell Signaling Technology), overnight at 4°C. Secondary antibodies included horseradish peroxidase (HRP)-conjugated anti-rat immunoglobulin G (Cell Signaling Technology) and HRP-conjugated anti-rabbit IgG (Cell Signaling Technology). Detection of protein bands was performed with an enhanced chemiluminescence (ECL) (Merck Millipore) substrate, and imaging was performed with ChemiDoc imaging systems (Bio-Rad). The immunoblots were quantified using ImageJ software, and results were normalized to β-actin expression.

Luminex assay. Corneal lysates or cell supernatants were assayed for the cytokines IFN-γ, IL-1α, IL-1β, IL-2, IL-4, IL-5, IL-6, IL-10, IL-12p40, IL-12p70, IL-15, IL-17, IP-10, M-CSF, and TNF-α using the Luminex kit according to the manufacturer's instructions (Milliplex multiplex assays with Luminex; Millipore Sigma, Danvers, MA). Samples were assayed using the Luminex assay system (Magpix).

Virus titration in eye swabs. Eye swabs (tears) were analyzed for viral titers by a plaque assay. RS cells were grown to 70% confluence in 24-well plates. The transfer medium in which eye swabs were stored was added after appropriate dilution at 250 μl per well in 24-well plates. Infected monolayers were incubated at 37°C for 1 h, rocked every 15 min for viral adsorption, and then overlaid with medium containing carboxymethyl cellulose. After 48 h of incubation at 37°C, cells were fixed and stained with crystal violet, and viral plaques were counted under a light microscope. Positive controls were run with every assay using previously determined viral titers of laboratory stocks of McKrae.

Statistical analysis. Data for each assay were compared by Student's *t* test using GraphPad Prism version 5 (GraphPad, La Jolla, CA). Differences between the groups were identified by analysis of variance (ANOVA) and multiple-comparison procedures, as we previously described (87). Data are expressed as the means ± standard deviations (SD). Results were considered statistically significant at a *P* value of ≤ 0.05.

SUPPLEMENTAL MATERIAL

Supplemental material is available online only.

SUPPLEMENTAL FILE 1, PDF file, 0.1 MB.

ACKNOWLEDGMENTS

This work is supported by Public Health Service research grants EY026103, EY019896, and EY024618 from the National Eye Institute (NEI) and grants AI143348, AI147499, AI143326, AI138764, AI124911, and AI110902 from the National Institute of Allergy and Infectious Diseases (NIAID) and in part by the Discovery Center for Eye Research (DCER) and a Research To Prevent Blindness (RPB) grant.

We thank Angele Nalbandian (Gavin Herbert Eye Institute, University of California, Irvine, Irvine, CA) for help editing the manuscript.

We declare that no conflict of interest exists.

REFERENCES

1. Looker KJ, Magaret AS, May MT, Turner KM, Vickerman P, Gottlieb SL, Newman LM. 2015. Global and regional estimates of prevalent and incident herpes simplex virus type 1 infections in 2012. PLoS One 10:1457–1465. https://doi.org/10.1371/journal.pone.0140765.
2. Awasthi S, Friedman HM. 2014. Status of prophylactic and therapeutic genital herpes vaccines. Curr Opin Virol 6:6–12. https://doi.org/10.1016/j.coviro.2014.02.006.
3. Srivastava R, Roy S, Coulon P-G, Vahed H, Prakash S, Dhanushkodi N, Kim GJ, Fouladi MA, Campo J, Teng AA, Liang X, Schaefer H, BenMohamed L. 2019. Therapeutic mucosal vaccination of herpes simplex virus 2-infected guinea pigs with ribonucleotide reductase 2 (RR2) protein boosts antiviral neutralizing antibodies and local tissue-resident $CD4^+$ and $CD8^+$ T_{RM} cells associated with protection against recurrent genital herpes. J Virol 93:e02309-18. https://doi.org/10.1128/JVI.02309-18.
4. Wald A, Link K. 2002. Risk of human immunodeficiency virus infection in herpes simplex virus type 2-seropositive persons: a meta-analysis. J Infect Dis 185:45–52. https://doi.org/10.1086/338231.
5. Vahed H, Agrawal A, Srivastava R, Prakash S, Coulon P-GA, Roy S, BenMohamed L. 2019. Unique type I interferon, expansion/survival cytokines, and JAK/STAT gene signatures of multifunctional herpes simplex virus-specific effector memory $CD8^+$ T_{EM} cells are associated with asymptomatic herpes in humans. J Virol 93:e01882-18. https://doi.org/10.1128/JVI.01882-18.
6. Samandary S, Kridane-Miledi H, Sandoval JS, Choudhury Z, Langa-Vives F, Spencer D, Chentoufi AA, Lemonnier FA, BenMohamed L. 2014. Associations of HLA-A, HLA-B and HLA-C alleles frequency with prevalence of herpes simplex virus infections and diseases across global populations: implication for the development of an universal CD8+ T-cell epitope-based vaccine. Hum Immunol 75:715–729. https://doi.org/10.1016/j.humimm.2014.04.016.
7. Farooq AV, Valyi-Nagy T, Shukla D. 2010. Mediators and mechanisms of herpes simplex virus entry into ocular cells. Curr Eye Res 35:445–450. https://doi.org/10.3109/02713681003734841.
8. West DM, Del Rosso CR, Yin XT, Stuart PM. 2014. CXCL1 but not IL-6 is required for recurrent herpetic stromal keratitis. J Immunol 192:1762–1767. https://doi.org/10.4049/jimmunol.1302957.
9. Carr DJ, Wuest T, Ash J. 2008. An increase in herpes simplex virus type 1 in the anterior segment of the eye is linked to a deficiency in NK cell infiltration in mice deficient in CXCR3. J Interferon Cytokine Res 28:245–251. https://doi.org/10.1089/jir.2007.0110.
10. Bouley DM, Kanangat S, Wire W, Rouse BT. 1995. Characterization of herpes simplex virus type-1 infection and herpetic stromal keratitis development in IFN-gamma knockout mice. J Immunol 155:3964–3971.
11. Suvas S, Azkur AK, Rouse BT. 2006. Qa-1b and CD94-NKG2a interaction regulate cytolytic activity of herpes simplex virus-specific memory CD8+ T cells in the latently infected trigeminal ganglia. J Immunol 176:1703–1711. https://doi.org/10.4049/jimmunol.176.3.1703.
12. Farr AR, Wu W, Choi B, Cavalcoli JD, Laouar Y. 2014. CD1d-unrestricted NKT cells are endowed with a hybrid function far superior than that of iNKT cells. Proc Natl Acad Sci U S A 111:12841–12846. https://doi.org/10.1073/pnas.1323405111.
13. Grubor-Bauk B, Arthur JL, Mayrhofer G. 2008. Importance of NKT cells in resistance to herpes simplex virus, fate of virus-infected neurons, and level of latency in mice. J Virol 82:11073–11083. https://doi.org/10.1128/JVI.00205-08.
14. Cornish AL, Keating R, Kyparissoudis K, Smyth MJ, Carbone FR, Godfrey DI. 2006. NKT cells are not critical for HSV-1 disease resolution. Immunol Cell Biol 84:13–19. https://doi.org/10.1111/j.1440-1711.2005.01396.x.
15. Fujita K, Sandford AP, Kobayashi M, Hanafusa T, Herndon DN, Suzuki F. 2005. Role of natural killer T (NKT) cells lacking interleukin (IL)-4 producing abilities on the CC-chemokine ligand 2-associated herpes simplex virus type 1 infection in human severe combined immunodeficiency (SCID) mouse chimeras. Burns 31:145–152. https://doi.org/10.1016/j.burns.2004.09.006.
16. Gill N, Rosenthal KL, Ashkar AA. 2005. NK and NKT cell-independent contribution of interleukin-15 to innate protection against mucosal viral infection. J Virol 79:4470–4478. https://doi.org/10.1128/JVI.79.7.4470-4478.2005.
17. Bendelac A. 1995. Positive selection of mouse NK1+ T cells by CD1-expressing cortical thymocytes. J Exp Med 182:2091–2096. https://doi.org/10.1084/jem.182.6.2091.
18. Bendelac A, Lantz O, Quimby ME, Yewdell JW, Bennink JR, Brutkiewicz RR. 1995. CD1 recognition by mouse NK1+ T lymphocytes. Science 268:863–865. https://doi.org/10.1126/science.7538697.
19. Bendelac A, Savage PB, Teyton L. 2007. The biology of NKT cells. Annu Rev Immunol 25:297–336. https://doi.org/10.1146/annurev.immunol.25.022106.141711.
20. Barral DC, Brenner MB. 2007. CD1 antigen presentation: how it works. Nat Rev Immunol 7:929–941. https://doi.org/10.1038/nri2191.
21. Sanderson JP, Brennan PJ, Mansour S, Matulis G, Patel O, Lissin N, Godfrey DI, Kawahara K, Zahringer U, Rossjohn J, Brenner MB, Gadola SD. 2013. CD1d protein structure determines species-selective antigenicity of isoglobotrihexosylceramide (iGb3) to invariant NKT cells. Eur J Immunol 43:815–825. https://doi.org/10.1002/eji.201242952.
22. Morita M, Motoki K, Akimoto K, Natori T, Sakai T, Sawa E, Yamaji K, Koezuka Y, Kobayashi E, Fukushima H. 1995. Structure-activity relationship of alpha-galactosylceramides against B16-bearing mice. J Med Chem 38:2176–2187. https://doi.org/10.1021/jm00012a018.
23. Seregin SS, Chen GY, Laouar Y. 2015. Dissecting CD8+ NKT cell responses to Listeria infection reveals a component of innate resistance. J Immunol 195:1112–1120. https://doi.org/10.4049/jimmunol.1500084.
24. Van Kaer L, Parekh VV, Wu L. 2015. The response of CD1d-restricted invariant NKT cells to microbial pathogens and their products. Front Immunol 6:226. https://doi.org/10.3389/fimmu.2015.00226.
25. Parekh VV, Wu L, Olivares-Villagomez D, Wilson KT, Van Kaer L. 2013. Activated invariant NKT cells control central nervous system autoimmunity in a mechanism that involves myeloid-derived suppressor cells. J Immunol 190:1948–1960. https://doi.org/10.4049/jimmunol.1201718.
26. Van Kaer L, Parekh VV, Wu L. 2011. Invariant natural killer T cells: bridging innate and adaptive immunity. Cell Tissue Res 343:43–55. https://doi.org/10.1007/s00441-010-1023-3.
27. Wu L, Gabriel CL, Parekh VV, Van Kaer L. 2009. Invariant natural killer T cells: innate-like T cells with potent immunomodulatory activities. Tissue Antigens 73:535–545. https://doi.org/10.1111/j.1399-0039.2009.01256.x.
28. Exley M, Garcia J, Balk SP, Porcelli S. 1997. Requirements for CD1d recognition by human invariant Valpha24+ CD4−CD8− T cells. J Exp Med 186:109–120. https://doi.org/10.1084/jem.186.1.109.
29. Benlagha K, Kyin T, Beavis A, Teyton L, Bendelac A. 2002. A thymic precursor to the NK T cell lineage. Science 296:553–555. https://doi.org/10.1126/science.1069017.
30. Carnaud C, Lee D, Donnars O, Park SH, Beavis A, Koezuka Y, Bendelac A. 1999. Cutting edge. Cross-talk between cells of the innate immune system: NKT cells rapidly activate NK cells. J Immunol 163:4647–4650.
31. Opasawatchai A, Matangkasombut P. 2015. iNKT cells and their potential lipid ligands during viral infection. Front Immunol 6:378. https://doi.org/10.3389/fimmu.2015.00378.

32. Grubor-Bauk B, Simmons A, Mayrhofer G, Speck PG. 2003. Impaired clearance of herpes simplex virus type 1 from mice lacking CD1d or NKT cells expressing the semivariant V alpha 14-J alpha 281 TCR. J Immunol 170:1430–1434. https://doi.org/10.4049/jimmunol.170.3.1430.
33. Sanchez DJ, Gumperz JE, Ganem D. 2005. Regulation of CD1d expression and function by a herpesvirus infection. J Clin Invest 115:1369–1378. https://doi.org/10.1172/JCI24041.
34. Rao P, Wen X, Lo JH, Kim S, Li X, Chen S, Feng X, Akbari O, Yuan W. 2018. Herpes simplex virus 1 specifically targets human CD1d antigen presentation to enhance its pathogenicity. J Virol 92:e01490-18. https://doi.org/10.1128/JVI.01490-18.
35. Gumperz JE, Miyake S, Yamamura T, Brenner MB. 2002. Functionally distinct subsets of CD1d-restricted natural killer T cells revealed by CD1d tetramer staining. J Exp Med 195:625–636. https://doi.org/10.1084/jem.20011786.
36. Krovi SH, Gapin L. 2018. Invariant natural killer T cell subsets—more than just developmental intermediates. Front Immunol 9:1393. https://doi.org/10.3389/fimmu.2018.01393.
37. Caielli S, Conforti-Andreoni C, Di Pietro C, Usuelli V, Badami E, Malosio ML, Falcone M. 2010. On/off TLR signaling decides proinflammatory or tolerogenic dendritic cell maturation upon CD1d-mediated interaction with invariant NKT cells. J Immunol 185:7317–7329. https://doi.org/10.4049/jimmunol.1000400.
38. Michel ML, Keller AC, Paget C, Fujio M, Trottein F, Savage PB, Wong CH, Schneider E, Dy M, Leite-de-Moraes MC. 2007. Identification of an IL-17-producing NK1.1(neg) iNKT cell population involved in airway neutrophilia. J Exp Med 204:995–1001. https://doi.org/10.1084/jem.20061551.
39. Lee YJ, Starrett GJ, Lee ST, Yang R, Henzler CM, Jameson SC, Hogquist KA. 2016. Lineage-specific effector signatures of invariant NKT cells are shared amongst gammadelta T, innate lymphoid, and Th cells. J Immunol 197:1460–1470. https://doi.org/10.4049/jimmunol.1600643.
40. Bennstein SB. 2017. Unraveling natural killer T-cells development. Front Immunol 8:1950. https://doi.org/10.3389/fimmu.2017.01950.
41. Thapa P, Manso B, Chung JY, Romera Arocha S, Xue HH, Angelo DBS, Shapiro VS. 2017. The differentiation of ROR-gammat expressing iNKT17 cells is orchestrated by Runx1. Sci Rep 7:7018. https://doi.org/10.1038/s41598-017-07365-8.
42. Tuttle KD, Krovi SH, Zhang J, Bedel R, Harmacek L, Peterson LK, Dragone LL, Lefferts A, Halluszczak C, Riemondy K, Hesselberth JR, Rao A, O'Connor BP, Marrack P, Scott-Browne J, Gapin L. 2018. TCR signal strength controls thymic differentiation of iNKT cell subsets. Nat Commun 9:2650–2655. https://doi.org/10.1038/s41467-018-05026-6.
43. Lee HK, Zamora M, Linehan MM, Iijima N, Gonzalez D, Haberman A, Iwasaki A. 2009. Differential roles of migratory and resident DCs in T cell priming after mucosal or skin HSV-1 infection. J Exp Med 206:359–370. https://doi.org/10.1084/jem.20080601.
44. Scheuplein F, Thariath A, Macdonald S, Truneh A, Mashal R, Schaub R. 2013. A humanized monoclonal antibody specific for invariant natural killer T (iNKT) cells for in vivo depletion. PLoS One 8:e76692. https://doi.org/10.1371/journal.pone.0076692.
45. Xu X, Pocock GM, Sharma A, Peery SL, Fites JS, Felley L, Zarnowski R, Stewart D, Berthier E, Klein BS, Sherer NM, Gumperz JE. 2016. Human iNKT cells promote protective inflammation by inducing oscillating purinergic signaling in monocyte-derived DCs. Cell Rep 16:3273–3285. https://doi.org/10.1016/j.celrep.2016.08.061.
46. Lee SW, Park HJ, Van Kaer L, Hong S, Hong S. 2018. Graphene oxide polarizes iNKT cells for production of TGFbeta and attenuates inflammation in an iNKT cell-mediated sepsis model. Sci Rep 8:10081. https://doi.org/10.1038/s41598-018-28396-9.
47. Fujii SI, Shimizu K. 2019. Immune networks and therapeutic targeting of iNKT cells in cancer. Trends Immunol 40:984–997. https://doi.org/10.1016/j.it.2019.09.008.
48. Halder RC, Tran C, Prasad P, Wang J, Nallapothula D, Ishikawa T, Wang M, Zajonc DM, Singh RR. 2019. Self-glycerophospholipids activate murine phospholipid-reactive T cells and inhibit iNKT cell activation by competing with ligands for CD1d loading. Eur J Immunol 49:242–254. https://doi.org/10.1002/eji.201847717.
49. Chandra S, Kronenberg M. 2015. Activation and function of iNKT and MAIT cells. Adv Immunol 127:145–201. https://doi.org/10.1016/bs.ai.2015.03.003.
50. Holzapfel KL, Tyznik AJ, Kronenberg M, Hogquist KA. 2014. Antigen-dependent versus -independent activation of invariant NKT cells during infection. J Immunol 192:5490–5498. https://doi.org/10.4049/jimmunol.1400722.
51. Kim EY, Lynch L, Brennan PJ, Cohen NR, Brenner MB. 2015. The transcriptional programs of iNKT cells. Semin Immunol 27:26–32. https://doi.org/10.1016/j.smim.2015.02.005.
52. Monteiro M, Graca L. 2014. iNKT cells: innate lymphocytes with a diverse response. Crit Rev Immunol 34:81–90. https://doi.org/10.1615/critrevimmunol.2014010088.
53. Lee DH, Jaggi U, Ghiasi H. 2019. CCR2+ migratory macrophages with M1 status are the early-responders in the cornea of HSV-1 infected mice. PLoS One 14:e0215727. https://doi.org/10.1371/journal.pone.0215727.
54. Gois BM, Peixoto RF, Maciel BLL, Gomes JAS, de Azevedo FLAA, Veras RC, de Medeiros IA, de Lima Grisi TCS, de Araújo DAM, do Amaral IPG, Keesen TSL. 2018. Dual immune effect of iNKT cells considering human cutaneous and visceral leishmaniasis: an example of cell plasticity according to different disease scenarios. Scand J Immunol 87:e12668. https://doi.org/10.1111/sji.12668.
55. Hayworth JL, Mazzuca DM, Maleki Vareki S, Welch I, McCormick JK, Haeryfar SM. 2012. CD1d-independent activation of mouse and human iNKT cells by bacterial superantigens. Immunol Cell Biol 90:699–709. https://doi.org/10.1038/icb.2011.90.
56. Askenase PW, Majewska-Szczepanik M, Kerfoot S, Szczepanik M. 2011. Participation of iNKT cells in the early and late components of Tc1-mediated DNFB contact sensitivity: cooperative role of gammadelta-T cells. Scand J Immunol 73:465–477. https://doi.org/10.1111/j.1365-3083.2011.02522.x.
57. Hirose S, Wang S, Tormanen K, Wang Y, Tang J, Akbari O, Ghiasi H. 2019. Roles of type 1, 2, and 3 innate lymphoid cells in herpes simplex virus 1 infection in vitro and in vivo. J Virol 93:e00523-19. https://doi.org/10.1128/JVI.00523-19.
58. Koujah L, Suryawanshi RK, Shukla D. 2019. Pathological processes activated by herpes simplex virus-1 (HSV-1) infection in the cornea. Cell Mol Life Sci 76:405–419. https://doi.org/10.1007/s00018-018-2938-1.
59. Wallace KL, Marshall MA, Ramos SI, Lannigan JA, Field JJ, Strieter RM, Linden J. 2009. NKT cells mediate pulmonary inflammation and dysfunction in murine sickle cell disease through production of IFN-gamma and CXCR3 chemokines. Blood 114:667–676. https://doi.org/10.1182/blood-2009-02-205492.
60. Sireci G, Russo D, Dieli F, Porcelli SA, Taniguchi M, La Manna MP, Di Liberto D, Scarpa F, Salerno A. 2007. Immunoregulatory role of Jalpha281 T cells in aged mice developing lupus-like nephritis. Eur J Immunol 37:425–433. https://doi.org/10.1002/eji.200636695.
61. Sonoda KH, Nakamura T, Young HA, Hart D, Carmeliet P, Stein-Streilein J. 2007. NKT cell-derived urokinase-type plasminogen activator promotes peripheral tolerance associated with eye. J Immunol 179:2215–2222. https://doi.org/10.4049/jimmunol.179.4.2215.
62. Exley MA, Hou R, Shaulov A, Tonti E, Dellabona P, Casorati G, Akbari O, Akman HO, Greenfield EA, Gumperz JE, Boyson JE, Balk SP, Wilson SB. 2008. Selective activation, expansion, and monitoring of human iNKT cells with a monoclonal antibody specific for the TCR alpha-chain CDR3 loop. Eur J Immunol 38:1756–1766. https://doi.org/10.1002/eji.200737389.
63. Yu S, Cantorna MT. 2008. The vitamin D receptor is required for iNKT cell development. Proc Natl Acad Sci U S A 105:5207–5212. https://doi.org/10.1073/pnas.0711558105.
64. Arshad MI, Rauch M, L'Helgoualc'h A, Julia V, Leite-de-Moraes MC, Lucas-Clerc C, Piquet-Pellorce C, Samson M. 2011. NKT cells are required to induce high IL-33 expression in hepatocytes during ConA-induced acute hepatitis. Eur J Immunol 41:2341–2348. https://doi.org/10.1002/eji.201041332.
65. Zheng Q, Zhou L, Mi QS. 2012. MicroRNA miR-150 is involved in Valpha14 invariant NKT cell development and function. J Immunol 188:2118–2126. https://doi.org/10.4049/jimmunol.1103342.
66. Wang J, Yang Q, Zhang Q, Yin C, Zhou L, Zhou J, Wang Y, Mi QS. 2017. Invariant natural killer T cells ameliorate monosodium urate crystal-induced gouty inflammation in mice. Front Immunol 8:1710. https://doi.org/10.3389/fimmu.2017.01710.
67. Lee SW, Park HJ, Cheon JH, Wu L, Van Kaer L, Hong S. 2018. iNKT cells suppress pathogenic NK1.1(+)CD8(+) T cells in DSS-induced colitis. Front Immunol 9:2168. https://doi.org/10.3389/fimmu.2018.02168.
68. Liu J, Gallo RM, Khan MA, Iyer AK, Kratzke IM, Brutkiewicz RR. 2019. JNK2 modulates the CD1d-dependent and -independent activation of iNKT cells. Eur J Immunol 49:255–265. https://doi.org/10.1002/eji.201847755.
69. Kulkarni RR, Villanueva AI, Read LR, Brisbin JT, Bhaumik SK, LaMarre J, Murali-Krishna K, Sharif S. 2017. CpG oligonucleotide-mediated costimulation of mouse invariant natural killer T cells negatively regulates

their activation status. Cell Tissue Res 369:541–554. https://doi.org/10.1007/s00441-017-2631-y.
70. Li L, Yang J, Jiang Y, Tu J, Schust DJ. 2015. Activation of decidual invariant natural killer T cells promotes lipopolysaccharide-induced preterm birth. Mol Hum Reprod 21:369–381. https://doi.org/10.1093/molehr/gav001.
71. Dong Q, Sugiura T, Toyohira Y, Yoshida Y, Yanagihara N, Karasaki Y. 2011. Stimulation of IFN-gamma production by garlic lectin in mouse spleen cells: involvement of IL-12 via activation of p38 MAPK and ERK in macrophages. Phytomedicine 18:309–316. https://doi.org/10.1016/j.phymed.2010.06.008.
72. Fukushima N, Nishiura Y, Nakamura T, Yamada Y, Kohno S, Eguchi K. 2005. Involvement of p38 MAPK signaling pathway in IFN-gamma and HTLV-I expression in patients with HTLV-I-associated myelopathy/tropical spastic paraparesis. J Neuroimmunol 159:196–202. https://doi.org/10.1016/j.jneuroim.2004.10.007.
73. He X, Jiang W, Luo Z, Qu T, Wang Z, Liu N, Zhang Y, Cooper PR, He W. 2017. IFN-gamma regulates human dental pulp stem cells behavior via NF-kappaB and MAPK signaling. Sci Rep 7:40681. https://doi.org/10.1038/srep40681.
74. Park WS, Jung WK, Park SK, Heo KW, Kang MS, Choi YH, Kim GY, Park SG, Seo SK, Yea SS, Liu KH, Shim EB, Kim DJ, Her M, Choi IW. 2011. Expression of galectin-9 by IFN-gamma stimulated human nasal polyp fibroblasts through MAPK, PI3K, and JAK/STAT signaling pathways. Biochem Biophys Res Commun 411:259–264. https://doi.org/10.1016/j.bbrc.2011.06.110.
75. Blahoianu MA, Rahimi AA, Kozlowski M, Angel JB, Kumar A. 2014. IFN-gamma-induced IL-27 and IL-27p28 expression are differentially regulated through JNK MAPK and PI3K pathways independent of Jak/STAT in human monocytic cells. Immunobiology 219:1–8. https://doi.org/10.1016/j.imbio.2013.06.001.
76. Tsao CC, Tsao PN, Chen YG, Chuang YH. 2016. Repeated activation of lung invariant NKT cells results in chronic obstructive pulmonary disease-like symptoms. PLoS One 11:e0147710. https://doi.org/10.1371/journal.pone.0147710.
77. Mathews S, Feng D, Maricic I, Ju C, Kumar V, Gao B. 2016. Invariant natural killer T cells contribute to chronic-plus-binge ethanol-mediated liver injury by promoting hepatic neutrophil infiltration. Cell Mol Immunol 13:206–216. https://doi.org/10.1038/cmi.2015.06.
78. Shiga Y, Sugamata R, Iwamura C, Nagao T, Zao J, Kawakami K, Kawachi S, Nakayama T, Suzuki K. 2014. Effect of invariant natural killer T cells with IL-5 and activated IL-6 receptor in ventilator-associated lung injury in mice. Exp Lung Res 40:1–11. https://doi.org/10.3109/01902148.2013.854518.
79. Doisne JM, Becourt C, Amniai L, Duarte N, Le Luduec JB, Eberl G, Benlagha K. 2009. Skin and peripheral lymph node invariant NKT cells are mainly retinoic acid receptor-related orphan receptor (gamma)t+ and respond preferentially under inflammatory conditions. J Immunol 183:2142–2149. https://doi.org/10.4049/jimmunol.0901059.
80. Smithgall MD, Comeau MR, Yoon BR, Kaufman D, Armitage R, Smith DE. 2008. IL-33 amplifies both Th1- and Th2-type responses through its activity on human basophils, allergen-reactive Th2 cells, iNKT and NK cells. Int Immunol 20:1019–1030. https://doi.org/10.1093/intimm/dxn060.
81. Divito SJ, Hendricks RL. 2008. Activated inflammatory infiltrate in HSV-1-infected corneas without herpes stromal keratitis. Invest Ophthalmol Vis Sci 49:1488–1495. https://doi.org/10.1167/iovs.07-1107.
82. Hendricks RL, Sugar J. 1984. Lysis of herpes simplex virus-infected targets. II. Nature of the effector cells. Cell Immunol 83:262–270. https://doi.org/10.1016/0008-8749(84)90305-8.
83. Iskeleli G, Camcioglu Y, Akova N, Kiran B, Bahar H, Deniz G. 2008. Lymphocyte subgroups and natural killer cell activity in recurrent herpetic stromal keratitis. Eye Contact Lens 34:169–173. https://doi.org/10.1097/ICL.0b013e318157a5c3.
84. Khan AA, Srivastava R, Chentoufi AA, Kritzer E, Chilukuri S, Garg S, Yu DC, Vahed H, Huang L, Syed SA, Furness JN, Tran TT, Anthony NB, McLaren CE, Sidney J, Sette A, Noelle RJ, BenMohamed L. 2017. Bolstering the number and function of HSV-1-specific CD8+ effector memory T cells and tissue-resident memory T cells in latently infected trigeminal ganglia reduces recurrent ocular herpes infection and disease. J Immunol 199:186–203. https://doi.org/10.4049/jimmunol.1700145.
85. BenMohamed L, Osorio N, Khan AA, Srivastava R, Huang L, Krochmal JJ, Garcia JM, Simpson JL, Wechsler SL. 2016. Prior corneal scarification and injection of immune serum are not required before ocular HSV-1 infection for UV-B-induced virus reactivation and recurrent herpetic corneal disease in latently infected mice. Curr Eye Res 41:747–756. https://doi.org/10.3109/02713683.2015.1061024.
86. BenMohamed L, Osorio N, Srivastava R, Khan AA, Simpson JL, Wechsler SL. 2015. Decreased reactivation of a herpes simplex virus type 1 (HSV-1) latency-associated transcript (LAT) mutant using the in vivo mouse UV-B model of induced reactivation. J Neurovirol 21:508–517. https://doi.org/10.1007/s13365-015-0348-9.
87. Jiang X, Brown D, Osorio N, Hsiang C, Li L, Chan L, BenMohamed L, Wechsler SL. 2015. A herpes simplex virus type 1 mutant disrupted for microRNA H2 with increased neurovirulence and rate of reactivation. J Neurovirol 21:199–209. https://doi.org/10.1007/s13365-015-0319-1.
88. National Research Council. 2011. Guide for the care and use of laboratory animals, 8th ed. National Academies Press, Washington, DC.